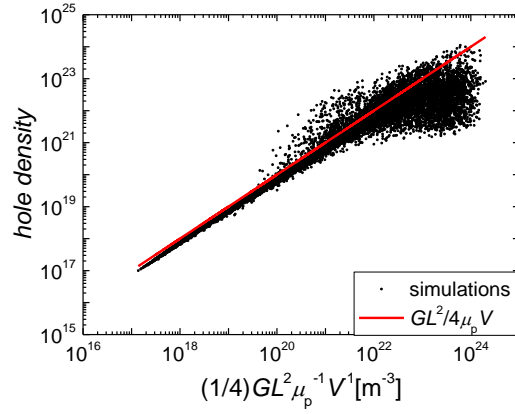
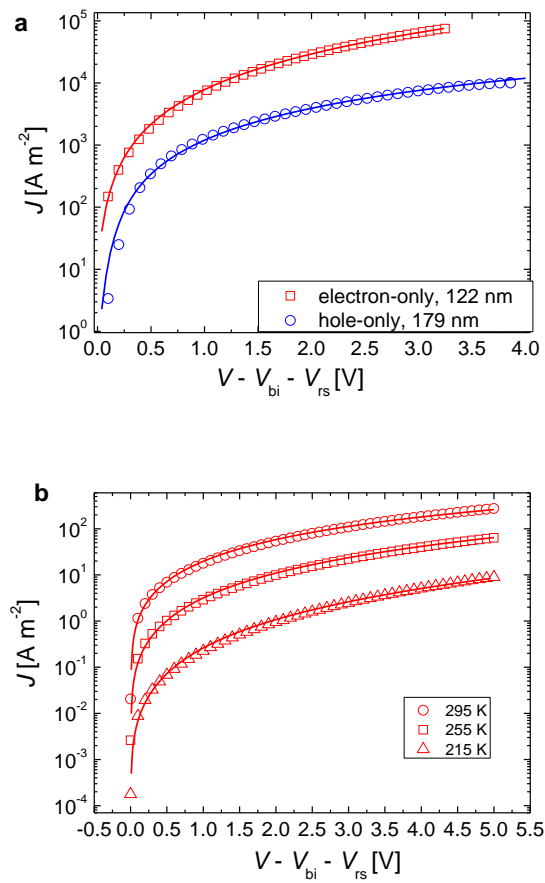


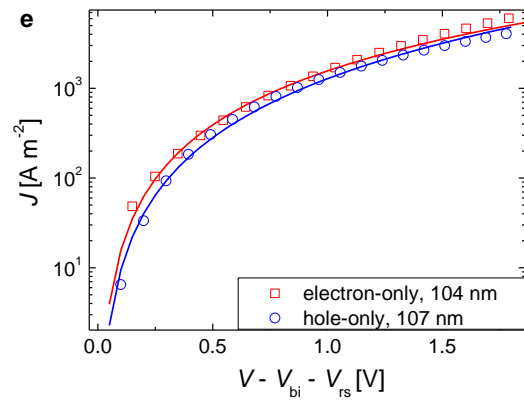
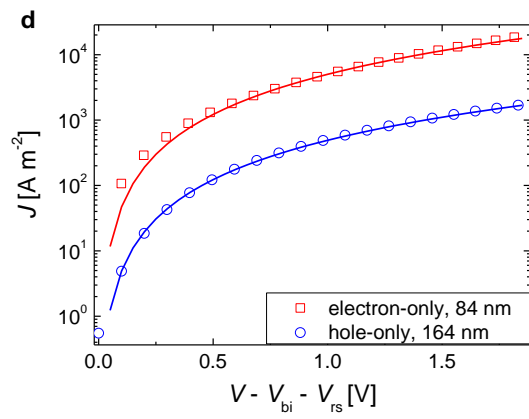
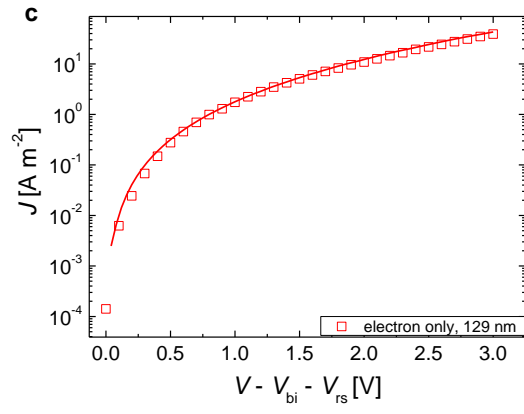
Supplementary Figure 1 (a) The effect of finite surface recombination (red symbols, $S_{n,p} = 10^{-4} \text{ m s}^{-1}$) and infinite surface recombination (black symbols). **(b)** Resulting fill-factors for $N_{cv} = 2.5 \times 10^{25} \text{ m}^{-3}$ (black) and $N_{cv} = 3 \times 10^{26} \text{ m}^{-3}$ (red).

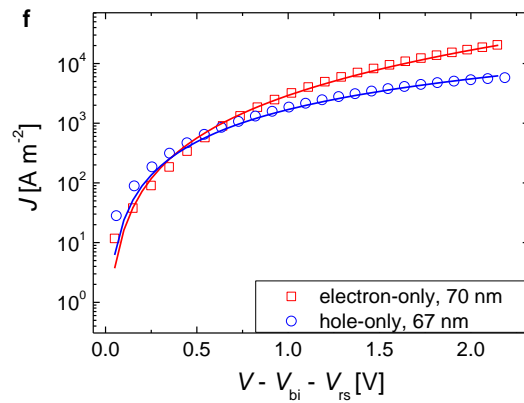


Supplementary Figure 2. Simulated density of holes at the cathode-side of the active layer as a function of $GL^2/\mu_p V_{\text{int}}$. The solid lines is calculated with the equation $p_{\text{av}} = \frac{GL^2}{4\mu_p V_{\text{int}}}$.

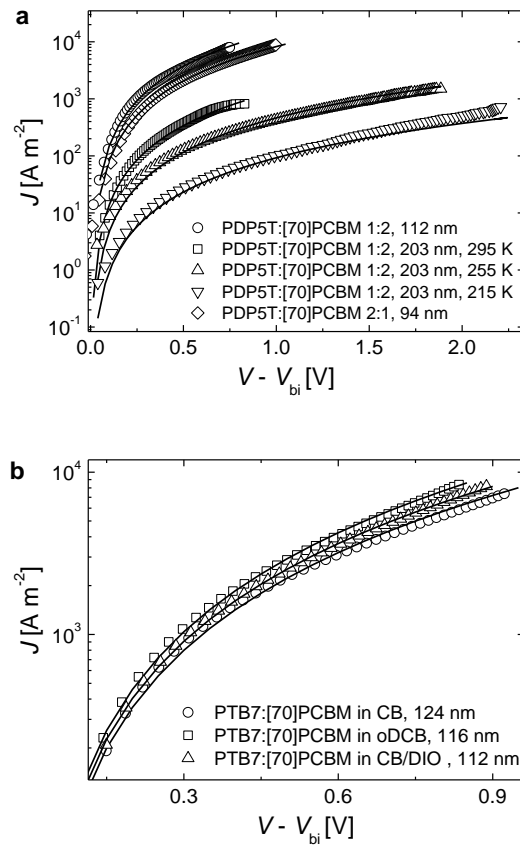
Supplementary Figure 3:



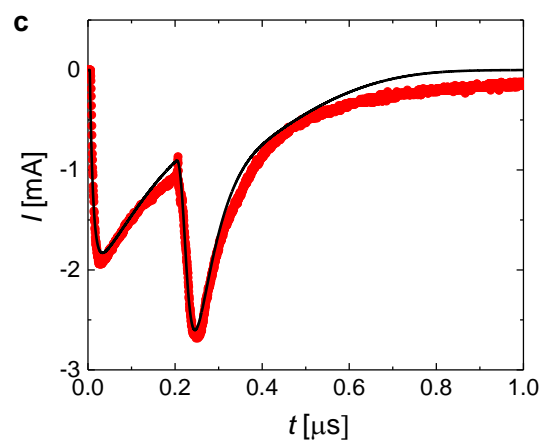
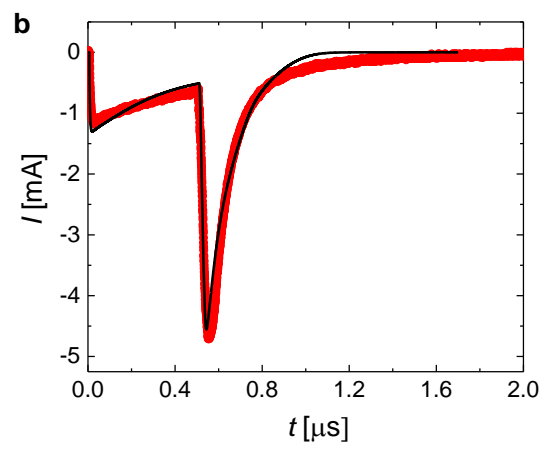
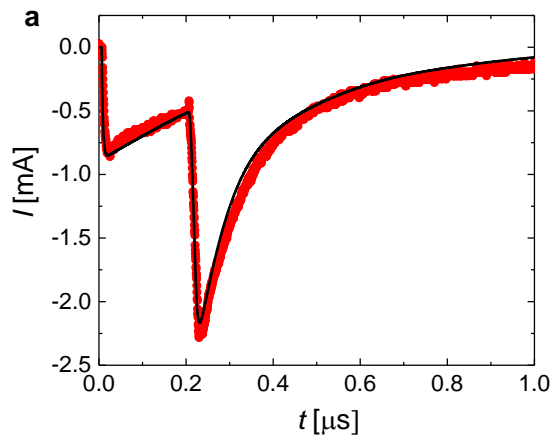


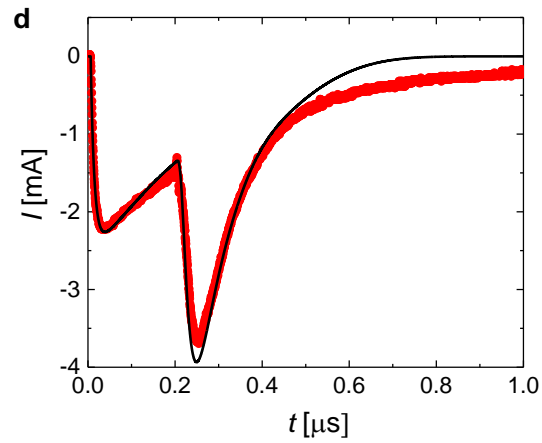


Supplementary Figure 3: J - V curves of PDPP5T:[70]PCBM and PTB7:[70]PCBM hole-only and electron-only devices. **(a)** PDPP5T:[70]PCBM 1:2 wt. ratio; **(b)** PDPP5T:[70]PCBM 1:1 wt. ratio; **(c)** PDPP5T:[70]PCBM 2:1 wt. ratio; **(d)** PTB7:[70]PCBM 1:1.5 wt. ratio from CB solution; **(e)** PTB7:[70]PCBM 1:1.5 wt. ratio from oDCB solution; **(f)** PTB7:[70]PCBM 1:1.5 wt. ratio from CB/DIO solution. Symbols represent experimental data, corrected for the series resistance of the substrates ($10 \text{ } \Omega/\text{square}$ for the electron-only devices, $14 \text{ } \Omega/\text{square}$ for the hole-only devices) and for the built-in voltage. Solid lines represent fit of the experimental data, performed for space charge limited current with a Poole-Frenkel dependency for the mobility on the electric field¹. The mobilities of holes and electrons are thus extracted as fit parameters from the J - V curves. For PDPP5T:[70]PCBM blends, the hole only was not measured for all the compositions; when the hole-only device was not fabricated, we got the hole mobility from a previous publication².

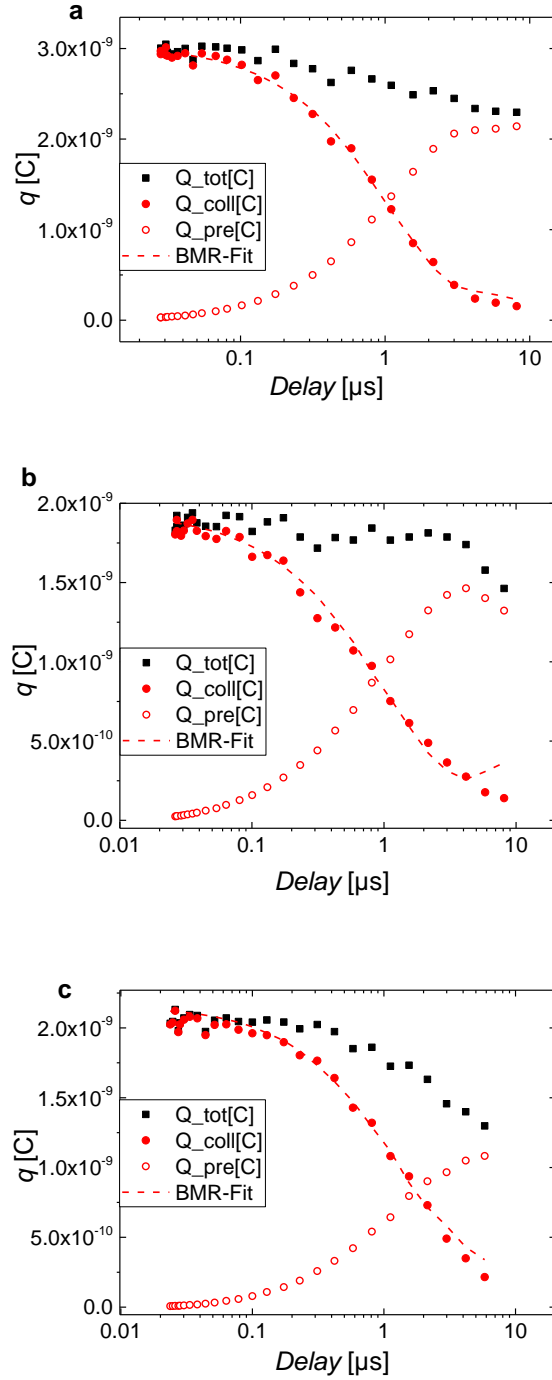


Supplementary Figure 4: J - V curves in dark for PDPP5T:[70]PCBM (a) and PTB7:[70]PCBM (b) solar cells. Symbols represent experimental data, solid lines represent fit of the experimental data.





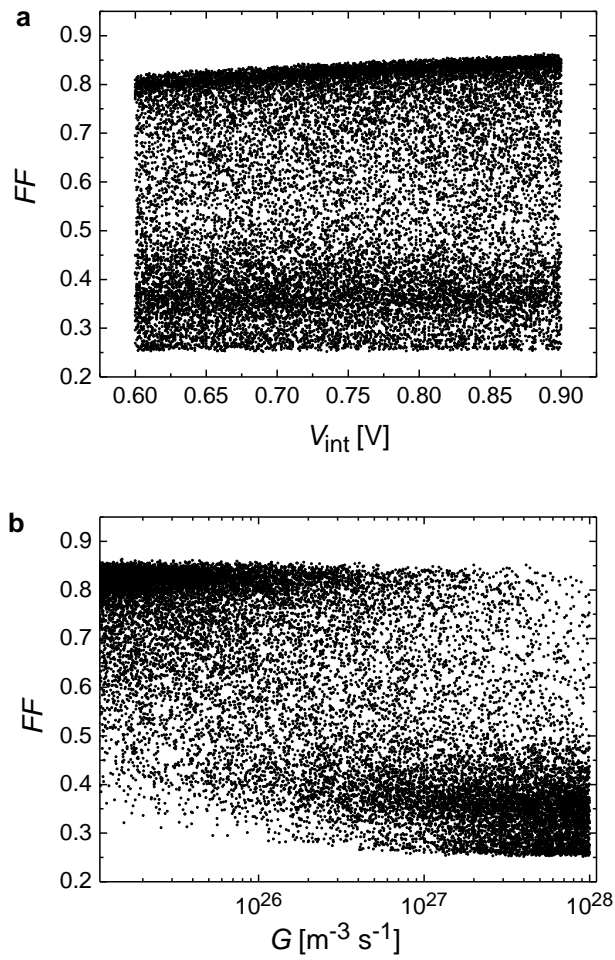
Supplementary Figure 5: TDCF transients of the polymer:polymer devices: P3HT:P(NDI2OD-T2) (a), P3HT:P(PDI2OD-T2) (b), POPT:P(NDI2OD-T2) (c), POPT:P(PDI2OD-T2) (d). The symbols represent experimental data, the solid lines represent fits with a numerical transient drift-diffusion simulation³⁻⁵.

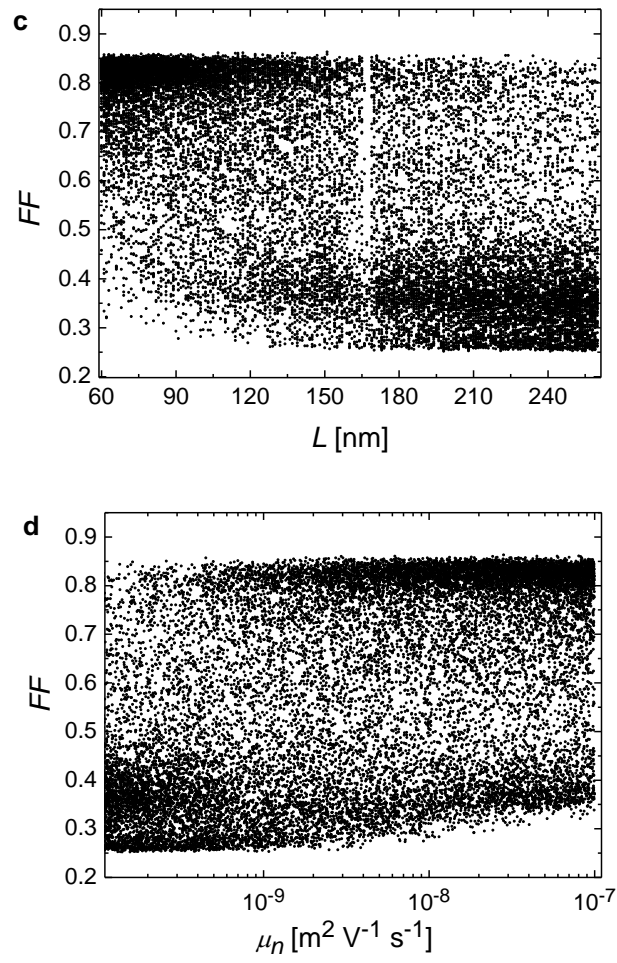


Supplementary Figure 6: Delay dependent total (Q_{tot} , black squares), collection (Q_{coll} , red full circles) and pre-charge (Q_{pre} , red empty circles) for P3HT:P(PDI2OD-T2) (a), POPT:P(NDI2OD-T2) (b) and POPT:P(PDI2OD-T2) (c). A pre-bias close to the maximum power point of each solar cell has been applied. The bimolecular recombination coefficients γ has been extracted from the fit of Q_{coll} with the equation²

$$Q_{\text{coll}}(t_D + \Delta t) = Q_{\text{coll}}(t_D) - [Q_{\text{pre}}(t_D + \Delta t) - Q_{\text{pre}}(t_D)] - \frac{\gamma}{eAd} [Q_{\text{coll}}^2(t_D) + 2Q_{\text{coll}}(t_D)Q_{\text{bg}}] \Delta t \quad (1)$$

Here, A and d are the device area and thickness, Q_{bg} is the background charge that arises due to dark injection from the contacts at forward bias.





Supplementary Figure 7: FF vs V_{int} (a), G (b), L (c) and μ_n (d) for the simulated data.

Supplementary Note 1 - Carrier densities at the contacts

In the case of thermal equilibrium at the contacts, it is assumed that the electron and hole density at the cathode ($x=0$) are equal to

$$n(0) = N_{cv} \quad (2)$$

$$p(0) = N_{cv} \exp\left(-\frac{E_g^{\text{eff}}}{kT}\right), \quad (3)$$

where N_{cv} is the density of available states [REFKoster2005], and E_g^{eff} is $LUMO_A - HOMO_D$.

At the anode the densities are given by

$$n(L) = N_{cv} \exp\left(-\frac{E_g^{\text{eff}}}{kT}\right) \quad (4)$$

$$p(L) = N_{cv} \quad (5)$$

In Ref. 6 it is assumed that $N_{cv} = 2.5 \times 10^{25} \text{ m}^{-3}$. If there is 1 hop site per 1.5 nm, then $N_{cv} = 3 \times 10^{26} \text{ m}^{-3}$.

In the case of near-zero surface recombination, the boundary conditions on $p(0)$ and $n(L)$ are replaced by the requirement that the hole, respectively, electron current densities are zero at cathode and anode. This is done by assuming

$$J_{n(p)} = qS_{np}(n(p) - n(p)_{\text{eq}}) \quad (6)$$

where S_{np} is the surface recombination velocity, where $n(p)_{\text{eq}}$ is the equilibrium electron (hole) density⁵. Near-zero recombination velocity is achieved by setting $S_{n,p} = 10^{-4} \text{ m/s}$.

Supplementary References

1. Frenkel, J. On pre-breakdown phenomena in insulators and electronic semiconductors. *Phys. Rev.* **54**, 647–648 (1938).
2. Bartesaghi, D., Turbiez, M., Koster, L. J. A. Charge transport and recombination in PDPP5T:[70]PCBM organic solar cells: the influence of morphology. *Org. Elect.* **15**, 3191–3202 (2014).
3. Albrecht, S., Janietz, S., Schindler, W., Frisch, J., Kurpiers, J., Kniepert, J., Inal, S., Pingel, P., Fostiropoulos, K., Koch, N. & Neher, D. Fluorinated copolymer PCPDTBT with enhanced open-circuit and reduced recombination for highly efficient polymer solar cells. *J. Am. Chem. Soc.* **134**, 14932–14944 (2012).
4. Roland, S., Schubert, M., Collins, B. A., Kurpiers, J., Chen, Z., Facchetti, A., Ade, H. & Neher, D. Fullerene-free polymer solar cells with highly reduced bimolecular recombination and field-independent charge carrier generation. *J. Phys. Chem. Lett.* **5**, 2815–2822 (2014).
5. Kniepert, J., Lange, I., van der Kaap, N. J., Koster, L. J. A. & Neher, D. A conclusive view on charge generation, recombination, and extraction in as-prepared and annealed P3HT:PCBM blends: combined experimental and simulation work. *Adv. Energy Mater.* **4**, 1301401 (2014).
6. Koster, L. J. A., Smits, E. C. P., Mihailetschi, V. D. & Blom, P. W. M. Device model for the operation of polymer/fullerene bulk heterojunction solar cells. *Phys. Rev. B* **72**, 085205 (2005).